Analytical Methods

Towards wearable fuel cell sensor for transdermal monitoring of isoflurane -an anesthetic

Complete List of Authors:	Jalal, Ahmed; Florida International University College of Engineering and Computing, Electrical and Computer Engineering Umasankar, Yogeswaran; Florida International University Department of Electrical and Computer Engineering, Biomolecular Sciences Institute Ahmed, Ashfaq; Florida International University College of Engineering and Computing, Biomedical Engineering Pretto, Jr. , Ernesto ; University of Miami School of Medicine, Anesthesiology, Miller School of Medicine Bhansali, Shekhar; Florida International University,

SCHOLARONE™
Manuscripts

Analytical Methods

Towards wearable fuel cell sensor for transdermal monitoring of isoflurane -an anesthetic

Ahmed Hasnain Jalal,[a†] Yogeswaran Umasankar,[b†] Md. Ashfaq Ahmed,[c] Ernesto A. Pretto Jr.[d] and Shekhar Bhansali[a]*

A miniaturized wearable platform with a micro-fuel cell sensor has been demonstrated for determination of isoflurane vapors from sweat. Principal component regression (PCR) was used to separate signals generated with changing isoflurane concentrations. The sensor was able to detect isoflurane vapor down to 40 ppm with a sensitivity of 0.038 nA ppm^{-1} cm^{-2} allowing for its use for physiological measurements. The results from PCR provided significant improvement in sensor calibration with ~81% minimization in deviation compared to linear calibration model. Our results demonstrate successful integration of a statistical technique (PCR model) and an analytical technique (fuel cell sensor) for physiologically relevant measurements of isoflurane- a standard anesthetic in surgical practices.

1. Introduction

Surgical procedures require 0.5 to 2% of an anesthetic agent with oxygen, air or nitrous oxide delivered through inhalation as an analgesic and to maintain sedation [1]. Isoflurane is one such anesthetic agent used commonly during surgery. An appropriate dose of the isoflurane is critical, a small variation in concentration can cause either an overdose or inadequate level of anesthesia resulting in awareness during surgery [2, 3]. Modern machines equipped with vaporizers and infrared spectroscopy (IR) sensors deliver the required dose of the isoflurane to maintain anesthesia throughout the surgery [4, 5]. In these complex machines, both

dispersive and nondispersive IR analyzers are being used to monitor the inhaled and exhaled isoflurane concentrations [5-8]. Examples of IR analyzers include ILCA2 from Drager, MIRAN SapphIRe model 205 BXL, photoacoustic transducer system from Brüel and Kjær 1302, and Capnomac from Dadex. These analyzers generally need a fully equipped hospital ambient environment to operate. They are expensive and most tend to encounter challenges when used in non-ideal environments [9]. Such machines find limited deployment for critical care in low resource environments due to issues of size, cost and complexity [9, 10], resulting in uncontrolled or poorly controlled administration of the anesthetic that in some instances results in negative health outcomes. An easy to use, low-cost anesthesia sensor has the potential to improve patient safety during surgical procedures in low-resource settings, improving both patient and health outcomes.

This work introduces a miniature, wearable, micro-fuel cell sensor capable of monitoring transdermal isoflurane. These micro-fuel cell sensors are the simplest form of the device composed of proton exchange membrane (PEM) sandwiched between metal electrodes. These sensors operate by simply generating current with respect to isoflurane concentration. However, existing IR analyzers has many optical components along with the sensor needing precise optical alignments. Unlike these fragile IR analyzers, micro-fuel cells are robust, small and can be deployed for field use at various environmental conditions. The data from the micro-fuel cell sensor can also be used to regulate vaporizers and ensure a controlled administration of an anesthetic like isoflurane for medical procedures.

Isoflurane (1-chloro-2,2,2-trifluoroethyl difluoromethyl ether) is a non-flammable volatile organic compound that undergoes minimal metabolism when ingested by humans and is excreted through breath (end-tidal), or through sensible and insensible perspiration [11, 12]. With minimal metabolism, the excreted concentrations of isoflurane are directly proportional

---

a. Electrical & Computer Engineering, Florida International University, Miami, Florida 33174, USA.

b. Biomolecular Sciences Institute, Florida International University, Miami, Florida 33174, USA.

c. Biomedical Engineering, Florida International University, Miami, Florida 33174, USA.

d. Anesthesiology, Miller School of Medicine, University of Miami, Miami, FL 33136, USA.

* sbhansa@fiu.edu † equal contribution.

COMMUNICATION

Journal Name

to the blood isoflurane concentrations [13]. Measuring transdermal isoflurane vapor emission and establishing its correlation with systemic isoflurane concentrations enables measurement of anesthesia levels in patients. In this study, the feasibility of measuring transdermal isoflurane concentrations in physiological range using the micro-fuel cell sensor has been investigated.

Under-resourced locations in many instances may have poor climate-controlled facilities. These changes in the environment negatively impact sophisticated instruments that are designed to operate in a controlled environmental range leading to significant variations in measured output over time. These multivariate environments disrupt chemical or biochemical sensor signals due to various intrinsic (e.g. hysteresis, fouling effect) and extrinsic ambient parameters (e.g. humidity, temperature, and other interferant compounds) [14, 15]. Thus, deviations in signals from the standard linear regression model tend to provide inaccurate readings over time during clinical measurements. Multivariate calibration methods, such as principal component regression (PCR) can address this limitation through reduction of redundancy of acquired data, leading to improved calibration [16]. PCR is a three-step calibration method, wherein the first step, redundancy is eliminated by principal component analysis (PCA), then the measured variable is transformed into latent variables, and lastly, a multiple linear regression step is performed between the scores of covariates obtained in PCA. This establishes an improved relationship between response variables and predictor variables. The other multivariate analyses such as PCA, discriminant function analysis (DFA) and linear discriminant analysis (LDA) can display only the training data in the subspace, but PCR can highly correlate larger data sets and improves fitting between known and unknown data. In this work, PCR was implemented to significantly improve the calibration of the micro-fuel cell sensor compared to the linear regression method.

2. Experimental

2.1. Materials and methods

The electrodes of a micro-fuel cell were nickel plated microperforated stainless-steel sheets (thickness 200 μm, pore

size 180 μm) [17]. Nafion N424 from Sigma Aldrich was used as a proton exchange membrane (PEM). Nickel sulphamate, nickel chloride anhydrous, boric acid, 95% sulfuric acid and 37% hydrochloric acid were purchased from Sigma-Aldrich. Lead and nickel sheets were purchased from McMaster-Carr for electroplating. Acetone, ethanol, and propanol (95.27%) were purchased from Fisher Scientific Inc. and acetonitrile (99.8%) was purchased from J. T. Baker. Isoflurane was purchased from Baxter healthcare corporation and Innovative Research. All other used chemicals were of analytical grade. Human sweat samples were collected following Institutional Ethical Guidelines (IRB-17-0300-AM01). Electrodeposition of nickel on stainless-steel sheets was achieved by Wood's Nickel Strike along with Watt's deposition method [18, 19]. A hydraulic hot press (model 2100 from PHI), was used to prepare the membrane electrolyte assembly (MEA) of the fuel cell sensor. Potentiostat CHI 1230B having MC470 was used for standard electrochemical testing. MATLAB was used to build a statistical model.

2.2 Micro-fuel cell sensor fabrication and calibration setup

The designed dimensions of the working electrode (WE), the counter electrode (CE) were 1 cm x 1 cm, and the reference electrode (RE) of the fuel cell sensor was 1 cm x 0.02 cm as shown in Figure 1a. Nafion (2 cm x 1 cm) was sandwiched between electrodes to form the MEA. The overall area of the CE was designed to be substantially larger than the WE and RE. The area of the RE was designed to contain the smallest surface area and it was placed at a specific distance from CE on the same side of the membrane. This distance (L= 0.55 cm) was kept three times ($L/\delta > 3$) greater than membrane thickness ($\delta = 0.02$ cm) to avoid the asymmetrical current distribution and potential variation on WE due to edging effect [20]. The sandwiched structure of MEA was achieved by hot pressing the MEA at 80 ˚C and 2500 psi for 10 min by a hydraulic press.

A chamber was used for sensor calibration, with the cathode exposed to atmospheric oxygen through a 1.5 cm x 1 cm opening. The WE was exposed to the atmosphere in the chamber through a 0.2 cm^2 window. During measurements, the chamber was filled with desired concentrations of isoflurane vapor. Specific vapor concentrations were attained by having concentrations of isoflurane solution at the bottom of the
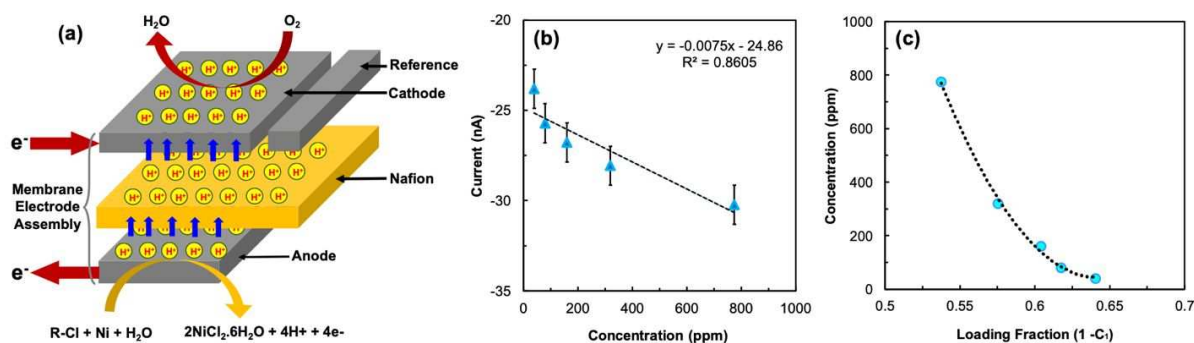
Figure 1. (a) Schematic of the micro-fuel cell sensor, (b) linear regression model and (c) PCR model of the sensor for isoflurane vapor.

chamber and allowing vapor to equilibrate to the solution concentrations. In this setup, the space between isoflurane solution and WE was maintained constant at the height of 0.2 cm, with total headspace volume of 0.4 cm^3. The isoflurane vapor concentrations in the headspace were controlled with the help of Henry's formula at constant temperature [21]. At 25 ˚C, the partition coefficient of isoflurane is 1.18 [22]. Various concentrations of isoflurane vapor 40 ppm, 80 ppm, 160 ppm, 320 ppm, and 775 ppm were exposed to WE and the corresponding signals were measured at the potential of -0.3V for sensor calibration. The same setup was used for isoflurane determination in human sweat.

2.3. Reaction mechanism

Oxidation and reduction reactions in fuel cell take place in anode and cathode respectively. Oxidative addition of isoflurane occurs in anode instead of direct isoflurane oxidation (Eq. 1 to 3), where R-Cl is the isoflurane.

$Ni + R\text{-}Cl \rightarrow RNi(II)^- + Cl^-$ (1)
$Cl_2 + H_2O \rightarrow HCl + HClO$ (2)
$4HCl + 2Ni + 12H_2O \rightarrow 2NiCl_2.6H_2O + 4H^+ + 4e^-$ (3)
$O_2 + 4H^+ + 4e^- \rightarrow 2H_2O$ (4)

The byproduct from the oxidative addition reaction (HCl in Eq. 3) gets oxidized on the anode and the electrons are transferred to the electrode. On cathode, the atmospheric oxygen gets reduced (Eq. 4) by getting those electrons from anode generating faradic current proportional to the concentration of isoflurane. In this process, H$^+$ ions flow from anode to cathode (Figure 1a). The generated faradic current was detected by the amperometric method.

3. Results and Discussion

3.1. Sensor signal overlaps in linear regression model

The linear response of the micro-fuel cell sensor was investigated with isoflurane vapor for five different concentrations, as mentioned earlier. The resulting data set had amperometric signals of these isoflurane vapor concentrations (Sec 2.2) at ambient temperature and humidity resulting in 8032 data points. Fitting the data in the linear regression model showed an increase in sensor signal with increasing isoflurane vapor concentration (Figure 1b) and had the sensitivity and coefficient of determination (R^2) value of 38 pA ppm^{-1} cm^{-2} and 86.05%, respectively. This relationship between the current response of the sensor with concentration as a variable had significant signal overlap between concentrations at nanoamperes. As an example, there was an overlap of 2.05 nA between 80 and 160 ppm, and 2.24 nA between 160 and 320 ppm. These signal overlaps lead to unreliable readings and poor selectivity between narrow ppm ranges especially as the sensitivity of the sensor is lower than the overlapping magnitude. The relative standard deviation (RSD) values for each concentration of 5.84, 5.77, 6.09, 6.76, and 10.62% also reveal significant deviations. The plausible causes of this signal overlap include (i) deviation of baseline over time, due to

change in H$^+$ ion counts in PEM, (ii) change in reaction rate of the electrodes due to transient fouling, (iii) slight variation in the ambient environment, such as humidity interference [23]. It would be impossible to control each variable of the measurement environment, so a linear regression model is not suitable for accurate isoflurane measurements. PCR model was investigated for the same dataset to improve the sensor calibration.

3.2. Sensor calibration for isoflurane vapor determination

PCR considers regressing outcomes of a set of covariates, which improves the accuracy compared to the linear regression model. PCR was executed by considering all the data points from the matrix of $D_{8032 \times 5}$, where the number of sample concentrations were 5 and the data points were 8032. In these calculations, the matrix was expressed in the form given in Eq. 5 [24].

$$D = RC \qquad (5)$$

where R and C are the scores and loading matrix, respectively. The eigenvalues (d), eigenvectors (V) and covariance matrix (Z) were directly related with the data matrix, D. To minimize the residual error, the eigenvectors were derived by subtracting d and V from Z. This iteration process was continued for eigenvectors till the eigenvalue reached below 0.001 of the maximum one. Eq. 7 was modified by employing a transformation matrix as R and C matrices, which do not exhibit any chemical and physical connotation. This transformation was executed as follows [24],

$$D = (RT)(T^{-1}C) \qquad (6)$$

T is a square matrix having with a dimension n and n is the number of significant factors which determined by PCR. This transformation matrix can be expressed as below,

$$T = \begin{vmatrix} x\cos(\delta) & -y\sin(\delta) \\ z\sin(\delta) & w\cos(\delta) \end{vmatrix} \qquad (7)$$

Values of the coefficient x, y, z, and w were unity when this matrix was orthogonal, else it was determined considering the information of the real factors. In this work, x = -2.5, y = 2, z = 5, w = 1, and δ = 351°. For regression fitting, loading fractions C_1 and 1-C_1 were determined empirically from PCR and fitted with respect to concentration of isoflurane as shown in Figure 1c. As all the experimental parameters are constant, the sum of the loading fractions was unity (1). Therefore, the regression plot was obtained from the plot of loading fraction (1-C_1) vs. concentration (y), where the R^2 value was obtained 99.77%. A polynomial function was fitted with the regression curve using MATLAB following the equation below.

$$x = \alpha(1 - C_1)^2 + \beta(1 - C_1) + \gamma \qquad (8)$$

The values of coefficient α, β, and γ were 1.789x10^4, -2.329x10^4, and 7.626x10^3, respectively. An unknown

concentration can be determined by fitting the loading fraction (1-C_1) in this regression model.
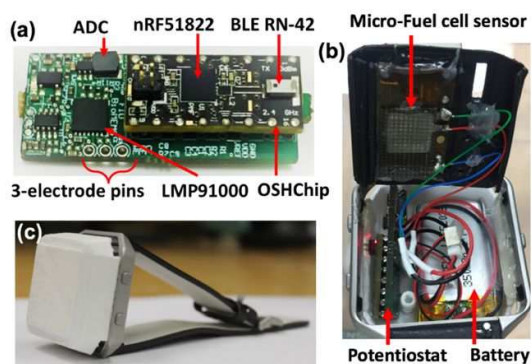
Figure 2. (a) Integrated PCB board and its components, (b) components of wearable watch and (c) wearable watch-prototype for isoflurane detection.

3.3. Miniaturized potentiostat for data collection

A wearable platform integrated with miniaturized potentiostat and micro-fuel cell sensor was built to measure transdermal isoflurane. A customized printed circuit board (PCB in Figure 2a) was designed to accommodate the low-cost potentiostat (LMP91000) with a low power data processing microcontroller nRF51822. This nRF5 series has a 32-bit ARM® Cortex™ M0 central processing unit (CPU) with 256kB/128kB flash + 32kB/16kB random access memory (RAM). The embedded 2.4GHz transceiver with nRF5 series support BLE for wireless data transmission and smartphone readout. Amperometry, an electrochemical measurement technique, was packaged in the

communication, and iii. amperometric operation. Since most of these operations only occur for a short period, the modules that run them were pushed to a lower power state, thereby reducing its consumption. The remaining time was utilized by the CPU to run other peripheral operations consuming ~ 2.6 µA at lower power. LMP91000, while in amperometric mode, consumed ~10 µA. It consumed an average current of ~7.95 µA over time with a total uptime of 39%. Including ~5 µA for cell conditioning, the current for this sensor was calculated as 9.75 µA with the LMP in 'stand mode' for 60% of the time. While the nRF51822 ran for ~5 seconds at a lower power from the CPU, the total power consumption was ~56 µW. Using a 3.7 V and 365 mAh Li-ion battery the operational lifetime of the system was ~ 5 days.

3.4. Measurement of isoflurane vapor from perspiration

In humans, a minimal percentage of isoflurane excretes through the skin by sensible and insensible perspiration [8]. This study was designed to determine the feasibility of the fuel cell sensor to measure the isoflurane vapor released from the sweat. The headspace of human sweat samples with various isoflurane concentrations was measured and compared with theoretical values to validate the sensor readings. Four different sweat solutions with isoflurane concentrations v/v%: 0.01%, 0.013%, 0.02%, and 0.038% respectively were tested. The theoretical isoflurane vapor concentrations were derived through Henry's formula [18]. The readings from the sensor were fitted with both linear regression and PCR models (Figure 3) to identify deviations from the theoretical values. Due to overlapping signals in the linear regression model, there was a significant deviation from theoretical values (~67.72%) resulting in low
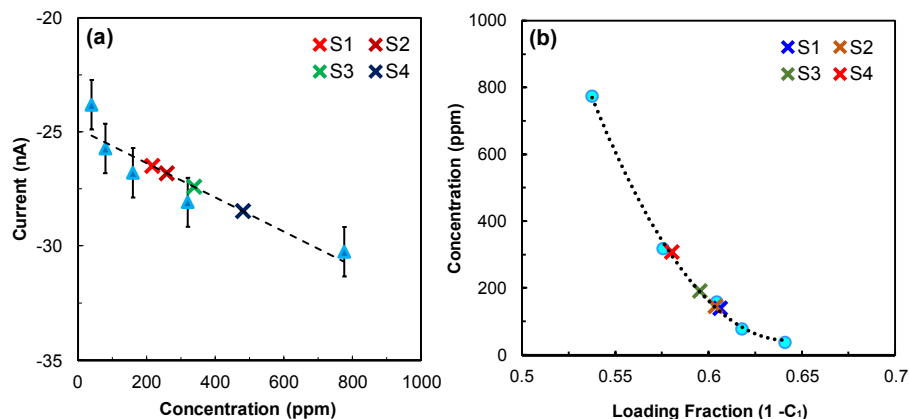
Figure 3. Isoflurane vapor signal from sweat samples fitted in regression models (a) linear regression and (b) PCR.

wearable form factor for isoflurane determination (Figure 2b and c). The steady-state amperometric current generated across WE and CE was measured by programming the potentiostat to bias -0.3 V across WE and RE. In this process, the signal from LMP91000 was converted into potential before feeding it to the internal analog-to-digital converter (ADC) and then to the microcontroller, where the data was processed in PCR model prior to data storage and display.

The power consumption of this device depended on: i. run time current drawn from the CPU, ii. BLE transmission and

resolution and inaccuracy (Table 1). The data from the PCR model improved compared to linear regression with a minimal deviation of about 12.74%. This ~81% improvement can be attributed to the consideration of covariates in the PCR model compared to linear regression. A student t-test was performed to validate the isoflurane results from the above two different calibration methods. The theoretical concentrations were used as reference values for the test. The results showed p (T<=t) values for linear regression and PCR as 0.0002 (< 0.05) and 0.65 (> 0.05), respectively. These p-values showed the null

COMMUNICATION

hypothesis was rejected in the case of linear regression and was not rejected in the case of PCR. This indicated that the difference in results between linear regression and theoretical calculation was statistically significant, and for PCR, the difference was not statistically significant. Hence, the PCR

results correlate with theoretical concentrations of isoflurane. Selectivity of the micro-fuel cell sensor for isoflurane has been investigated by the amperometric method in presence of major organic volatile compounds (VOC) generated from the skin. The VOCs include ethanol, acetone, propanol, and acetonitrile. Each of these compounds was exposed to the sensor during isoflurane measurements after the sensor reached steady-state. The VOC concentrations tested were the highest concentrations found in healthy subjects. The results show that there was a change in isoflurane signal with about 4.65%, 4.59%, 0.22% and 0.66% deviation in presence of ethanol, acetone, propanol, and acetonitrile respectively (Figure 4). The interference from the mixture of all four VOCs showed only about 2.4% of deviation in the signal. All these above results show the micro-fuel cell sensor along with PCR fitting can be used to determine the isoflurane vapor concentrations from the sweat. The advantages of micro-fuel cell sensor compared to the existing devices for isoflurane measurements have been discussed in Table 2. Even though the spectroscopic methods can detect lower concentrations and wider range, there is no known wearable transdermal sensor available for isoflurane measurements which is small enough and can detect isoflurane from skin perspiration.

Figure 4. Amperometric signal of the micro-fuel cell sensor for isoflurane (100 ppm) in presence of interfering compounds ethanol (1.5 ppm), acetone (0.8 ppm), propanol (0.15 ppm) and acetonitrile (0.1 ppm).

Table 1. Comparison of linear regression with PCR model for isoflurane detection from sweat.

Sample	Theoretical (ppm)	Linear regression (ppm)	Deviation (%)	PCR (ppm)	Deviation (%)
S1	112.00	216.91	93.67	141.59	26.42
S2	144.00	258.24	79.33	147.36	02.33
S3	216.00	338.4	56.66	192.63	10.82
S4	350.00	480.24	37.21	310.08	11.41

Table 2. Comparison of different sensing techniques for isoflurane detection.

Methods	Source	Lowest concentration	Advantage	Limitations	Reference
Gas chromatography with flame-ionization detector (FID)	Blood	< 0.1 ppm	Accurate, real-time and continuous monitoring	Not portable	25
Photoacoustic IR spectrometer	Breath	0.01 ppm with an accuracy of ~2%	Accurate, real-time and continuous monitoring	Not portable	7
Infrared spectrophotometer (MIRAN 205B Series SapphIRe-XL)	Breath	0.05 ppm (with an accuracy of +/− 10%)	Portable, Moderate accuracy, real-time and continuous monitoring	Not wearable	26
Isoflurane monitoring badge	Air	< 2 ppm	Wearable	Used for occupational exposure. Accuracy requirements at both 8-hour TWA,[a] required additional time and data analyst	27
Micro-fuel cell sensor	Skin perspiration	40 ppm	Wearable, real-time, continuous monitoring, covers physiological range	Moderate accuracy, 5% interference from other VOCs	This work

[a]Time-Weighted Average (TWA)

4. Conclusions

A micro-fuel cell sensor device was successfully implemented for the determination of transdermal isoflurane. The isoflurane vapor concentrations derived from PCR correlated with theoretical values compared to the linear regression model. PCR enabled isolation of signals in the nanoampere range and improved resolution of the signal on an average of five times compared to the linear regression. PCR accurately classified and discriminated different concentrations of isoflurane within the physiological range [28]. The low powered electronics of this was operational for 5 days after a single charge. This work demonstrates a potential system for determining isoflurane levels.

Acknowledgment

Conflicts of interest

There are no conflicts to declare.

References

1   P. Flecknell, J. L. S. Lofgren, M. C. Dyson, R. R. Marini, M. M. Swindle, R. P.Wilson, "Preanesthesia, Anesthesia, Analgesia, and Euthanasia," Laboratory Animal Medicine , pp. 1135-1200, 2015.

2   L. T. D. Duarte, G. F. D. Neto and F. F. Mendes, "Nitrous oxide use in children," Rev. Bras. Anestesiol, vol. 62, no. 3, pp. 451-467, 2012.

3   S. E. Dohoo, "Isoflurane as an inhalational anesthetic agent in clinical practice," Can Vet J., vol. 31, no. 12, pp. 847–850, 1990.

4   J. F. A. Hendrickx, H. J. M. Lemmens, R. Carette, A. M. D Wolf, L. J. Saidman, "Can modern infrared analyzers replace gas chromatography to measure anesthetic vapor concentrations?" BMC Anesthesiology, vol. 8, no. 2, pp. 1-6, 2008.

5   A. Sharma, G. Biyani, and R.Ramachandran, "Factitious reading by gas monitor," J Anaesthesiol Clin Pharmacol., vol. 32, no. 4, pp. 530–532, 2016.

6   Andrea R. Mulvenon, "Occupational exposure to isoflurane anesthetic gas in the research environment," Ph.D. Dissertation, University of Nebraska Medical Center, 2015.

7   K. H. Hoerauf, C. Koller, W. Jakob, K. Taeger and J Hobbhahn, "Isoflurane waste gas exposure during general anaesthesia: the laryngeal mask compared with tracheal intubation," Brit. J. of Anaesth., vol. 77 (2), pp. 189–193, 1996.

8   B. Walder, R. Lauber, A. M Zbinden, "Accuracy and cross-sensitivity of 10 different anesthetic gas monitors," J Clin Monit. Vol. 9, no. 5, pp. 364-73, 1993.

9   S. Lewis, and S. Jagdish, "Combat Anesthesia: The First 24 Hours," Chapter 15, pp. 181-190, 2016.

10 I. A. Walker, T. Bashford, J. E. Fitzgerald, I. H. Wilson, "Improving Anesthesia Safety in Low-Income Regions of the World," Curr. Anesthesiol. Rep., vol. 4, pp. 90–99, 2014.

11 S. H. Lockhart, N. Yasuda, N. Peterson, M. Laster, S. Taheri, R. B. Weiskopf, E. I. Eger, "Comparison of percutaneous losses of sevoflurane and isoflurane in humans," Anesthesia & Analgesia, vol. 72, no. 2, pp. 212–215, 1991.

12 C.-C. Lu, C.-S. Tsai, O. Y.-P. Hu, R.-M. Chen, T.-L. Chen, S. T. Ho, "Pharmacokinetics of isoflurane in human blood, Pharmacology," vol. 81, pp. 344–349, 2008.

13 R. Jacob. B. S. Krishnan, T Venkatesan, "Pharmacokinetics and pharmacodynamics of anesthetic drugs in pediatrics," Indian J. Anaesth., vol. 48, No. 5, pp. 340-346, 2004.

14 Y. Wang, D. J. Veltkamp, B. R. Kowalski, "Multivariate instrument standardization," Anal. Chem., vol. 63, No. 23, pp. 2750–2756, 1991.

15 A. H. Jalal, Y. Umasankar, P. J. Gonzalez, A. Alfonso, S. Bhansali, "Multimodal technique to eliminate humidity interference for specific detection of ethanol," Biosensors and Bioelectronics, vol. 87, pp. 595-608, 2017.

16 H. Cardot, C. Goga, and M.-A. Shehzad, Calibration and partial calibration on principal components when the number of auxiliary variables is large," Statistica Sinica, vol. 27, pp. 243-260, 2017.

17 A. H. Jalal, Y. Umasankar, S Bhansali, "Development and characterization of fuel cell sensor for potential transdermal ethanol sensing," ECS Transections, vol. 72, No. 31, pp. 25-31, 2016.

18 J. W. Dini, "Plating on Invar, VascoMax C-200, and 440C stainless steel," Surface and Coatings Technology, vol. 78, pp. 14-18, 1996.

19 O. P. Watts, "Rapid Nickel Plating," Am. Electrochem. Soc., Trans. Vol. 29, pp. 395-400,1916.

20 A. A. Kulikovsky, P. Berg, "Positioning of a reference electrode in a PEM fuel cell," J. of The Electrochem. Soc., vol. 162, no. 8, pp. F843–F848, 2015.

21 K. M. Dubowski, "Breath-alcohol simulators: scientific basis and actual performance," J. of analytical toxicology, vol. 3, pp. 177-182, 1979.

22 W. Honemann, J. Washington, M. C. Honemann, G. W. Nietgen and M. E. Durieux, "Partition Coefficients of Volatile Anesthetics in Aqueous Electrolyte Solutions at Various Temperatures," Anesthesiology, vol. 89, pp. 1032-1035, 1998.

23 S. Kim, I. Hong, "Effects of humidity and temperature on a proton exchange membrane fuel cell (PEMFC) stack," *J. Industrial and Engineering Chem.*, vol. 14, pp. 357–364, 2008.

24 M. E. Kose, A. Omar, C. A. Virgin, B. F. Carroll and K. S. Schanze, "Principal component analysis calibration method for dual-luminophore oxygen and temperature sensor films: application to luminescence imaging," Langmuir, vol. 21, pp. 9110–9120, 2005.

25 T. Kojima, A. Ishii, K. Watanabe-Suzuki, R. Kurihara, H. Seno, T. Kumazawa, O. Suzuki and Y. Katsumata, "Sensitive determination of four general anaesthetics in human whole blood by capillary gas chromatography with cryogenic oven

Analytical Methods

COMMUNICATION

trapping," Journal of Chromatography B, vol. 762, pp. 103–108, 2001.

26 K. R. Johnstone, C. Lau and J. L. Whitelaw, "Evaluation of waste isoflurane gas exposure during rodent surgery in an Australian university," J. of Occup. and Environ. Hygiene, vol. 14, pp. 955 – 964, 2017.

27 J. M. Elmer, "An Analytical Comparison of Isoflurane Levels in Veterinary Operating Theaters," Master's Project, School of Public Health, Drexel University, pp. 1- 19, 2010.

28 T. Lin, C. Lu, C.Hsu, J. V. Pergolizz Jr, C. Chang, M. Lee, S. Ho, "Awakening arterial blood and end-tidal concentrations of isoflurane in female surgical patients," Medicine, vol. 95, no. 30, pp. 1 -6, 2016.

Table of Content

H_2O O_2

e^-

e^-

R-Cl + Ni + H_2O $2NiCl_2.6H_2O + 4H^+ + 4e^-$
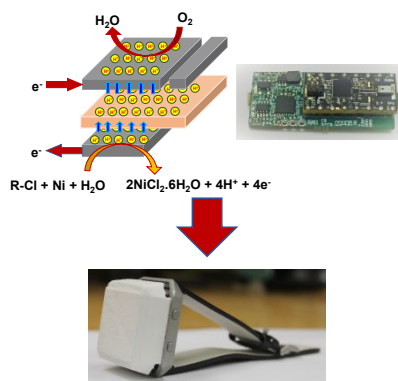
The wearable anesthesia sensor combines with principal component regression as a new approach in the analytical field for improving accuracy.